Proceedings of the 11th ICPMG 2026
11th International Conference on Physical Modelling in Geotechnics
8-12 June 2026, Zurich, Switzerland

Centrifuge Modeling of Saturated Mine Waste Rock Under Cyclic Loading

I. Sasanakul
University of South Carolina, Columbia, USA, sasanaku@cec.sc.edu

P. Ruttithivaphanich
Jacobs, Seattle, USA Country, Pitak.Rutti@jacobs.com

S. Dejphumee
Schnabel Engineering, City, West Columbia, USA, sdejphumee@schnabel-eng.com

ABSTRACT: This study investigates the dynamic response of mine waste rock with two different gravel-to-sand compositions using centrifuge model tests conducted at the University of South Carolina's geotechnical centrifuge facility. Two mixtures with gravel-to-sand ratios of 2.33:1 and 4:1 by weight were prepared with the same initial void ratio but result in different relative densities. Uniform cyclic loading was applied with peak base accelerations of 0.286 g and 0.210 g for the 2.33:1 and 4:1 mixtures, respectively. Despite the difference in shaking amplitude, both models experienced a similar cyclic stress ratio (CSR) of approximately 0.30 at the base. The 2.33:1 mixture generated higher excess pore water pressure, larger cyclic shear strains, and greater volumetric strain, indicating a more pronounced reduction in stiffness and strength. Excess pore water pressure in this mixture accumulated during the initial loading cycles and partially dissipated as shaking continued. Although both mixtures exhibited dilative behavior at low effective stress, their pore water pressure responses differed markedly. The 4:1 mixture developed excess pore water pressure that dissipated within each cycle without residual accumulation, reflecting a more stable cyclic response. In contrast, the 2.33:1 mixture developed excess pore water pressure of greater magnitude and accumulation and experienced more than twice the volumetric strain of the 4:1 mixture. These results demonstrate that gravel-to-sand ratio strongly influences the dynamic behavior of mine waste rock. Relatively small changes in particle composition significantly affect pore pressure generation, accumulation and dissipation behavior, deformation characteristics, and seismic stability, highlighting the importance of optimizing particle gradation and mixing to improve the seismic performance of mine waste embankments.

1 INTRODUCTION

Physical composition of mine waste rock, consisting of angular particles ranging from boulders to fine sands, creates a challenge in laboratory element tests due to the lack of large-scale equipment. Currently, limited studies on dynamic properties and behaviors of mine waste rock are available in literature, which in turn impacts the design and performance evaluation of existing tailings and mine waste facilities. Dynamic centrifuge modeling is a powerful tool to overcome the problem as a model of large particle samples can be dynamically loaded under a centrifuge gravitational acceleration to simulate earthquake loading and field stress conditions. Several centrifuge studies have been conducted to evaluate consolidation process and dynamic behaviors of tailings, waste rock, and co-mixing of tailings and waste rock (e.g. Antonaki et al., 2017, 2018; Sorta 2015; Salam 2020; Ruttithivaphanich and Sasanakul 2022, 2023). Antonaki et al. (2017, 2018) conducted a series of centrifuge modeling tests to investigate consolidation behavior and dynamic response of tailings and waste rock co-disposal with tailings. Ruttithivaphanich and Sasanakul (2022, 2023) observe liquefaction behaviors of waste rock samples with different compositions. These studies show that centrifuge modeling has a potential to provide a large set of meaningful experimental data to support tailings and mine waste facility projects.

This paper presents centrifuge modeling tests to investigate dynamic response of waste rock samples subjected to cyclic loading. The particle size of these samples is typically too large to conduct in a standard cyclic triaxial or cyclic simple shear test device. These samples have two different ratios of gravel to sand particles with no fine content. Two centrifuge models were prepared for each sample under a loose saturated condition and were subjected to self-weight consolidations under a 50-g centrifugal acceleration followed by cyclic loading. Centrifugal acceleration generates field stress conditions simulating a waste rock profile of 8 m in depth. While the shaking amplitudes applied to both models were not high enough to manifest liquefaction, excess pore water pressure, and volumetric strain were observed in both models. Differences in model behaviors are compared to assess the effects of soil composition.

2 MATERIAL AND CENTRIFUGE TEST PREPARATION

This study compares the dynamic response of two waste rock samples with different gravel-to-sand ratios. The first sample, designated as Sample 2.33:1, consists of 70% gravel and 30% sand by weight, while the second sample, designated as Sample 4:1, consists of 80% gravel and 20% sand by weight. Both samples contain no particles smaller than 0.075 mm, and the maximum particle size is less than 20 mm. The grain size distribution curves for both samples, along with a photograph of the materials, are presented in Figure 1. The particle shapes of both gravel and sand were visually classified as angular in accordance with ASTM D2488.

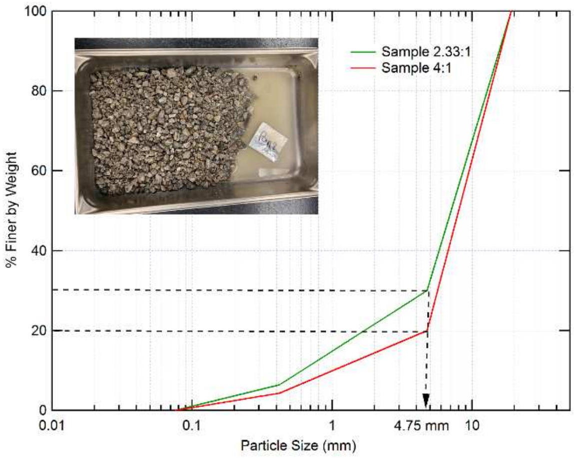

Figure 1. Grain Size Distribution Curve of Test Soil

The samples were prepared in a centrifuge laminar container with dimensions shown in Figure 2. The centrifuge models were instrumented with pore water pressure transducers, accelerometers, and linear variable displacement transducers (LVDTs). The model was divided into four layers, with each layer instrumented with a pair of pore water pressure transducers and accelerometers, while an LVDT was installed at the surface of the model. The samples were prepared using a moist tamping technique under very loose conditions, with an initial dry unit weight of 15.7 kN/m³. Saturation was achieved using a viscous fluid with a viscosity of 50 cP to maintain prototype soil permeability under a centrifugal acceleration of 50 g. The model was then installed on the centrifuge shaker and spun up to 50 g for consolidation and subsequent shaking.

Prior to shaking, the initial void ratio and relative density (Dr) of both models were evaluated using settlement measurements to establish the initial model conditions. These results are summarized in Table 1. Both models exhibited the same initial void ratio but different relative densities, which is attributed to the influence of material composition on the maximum and minimum void ratios.

A 1 Hz uniform sinusoidal waveform was applied as the input shaking motion to the centrifuge shaker. The measured shaker response is presented in Figure 3. Model 2.33:1 was subjected to cyclic loading with an average base shaking amplitude of 0.286 g for 40 cycles, whereas Model 4:1 was subjected to an average base shaking amplitude of 0.210 g for 15 cycles. The longer shaking duration applied to Model 2.33:1 was intended to induce liquefaction and to evaluate the effect of the number of loading cycles on the sample response.

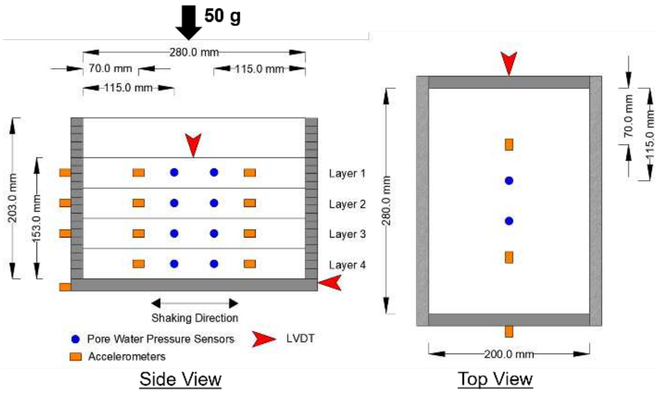

Figure 2. Schematic of the centrifuge model

Table 1. Initial Properties

Initial Condition Prior to Shaking	Sample 2.33:1	Sample 4:1
Void Ratio, e*	0.685	0.686
e_{max}, e_{min}	0.721, 0.5	0.754, 0.518
Dr (%)	16.3	28.6

* Calculated based settlement measurement at 50 g and assumed G_s = 2.7

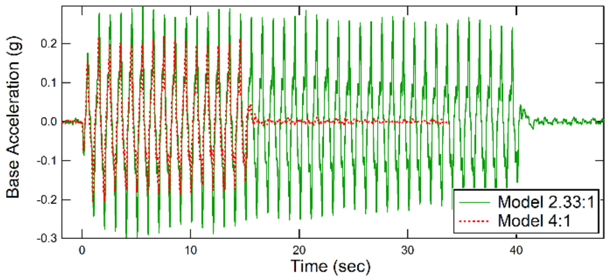

Figure 3. Time Histories of Input Motion

3 TEST RESULTS

Each dynamic centrifuge test produced time histories of acceleration and pore water pressure at multiple depths within the model. These measurements enabled analysis of the soil response in terms of effective stress. The base shaking acceleration applied by the centrifuge shaker was also recorded and analyzed. The acceleration time histories were subsequently used to compute shear stress and shear strain within the model following the procedure proposed by Zeghal and Elgamal (1996), which has been widely adopted in dynamic centrifuge studies (e.g., Brennan et al., 2005; Elgamal et al., 2005; Rayhani and Naggar, 2008). Surface settlements were measured using LVDTs and were employed to evaluate the average volumetric response of the model during shaking. In this section, the cyclic stress ratio and the corresponding cyclic shear strain are evaluated. Subsequently, the evolution of volume change and excess pore water pressure with increasing number of loading cycles is presented.

3.1 Cyclic Stress and Strain Response

3.1.1 Cyclic shear stress ratio (CSR)

Figure 4 presents the time histories of the cyclic stress ratio (CSR), defined as the ratio of shear stress to vertical effective stress, generated at different depths in both models. For Model 2.33:1, the CSR time histories are less uniform than those of Model 4:1, particularly in the upper half of the model. This behavior is likely attributable to a greater reduction in stiffness and strength in Model 2.33:1 during the initial shaking cycles. As the number of shaking cycles increases, pronounced spikes in the CSR response are observed in the upper half of the model.

In contrast, at the bottom layer (Layer 4), where the effective vertical stress is approximately 60 kPa, the CSR time histories are relatively uniform, indicating that both soil models were able to sustain most of the shear stress transmitted from the base shaking. At this depth, the average CSR values for Model 2.33:1 and Model 4:1 are comparable (0.30 and 0.32, respectively), despite the difference in base shaking amplitudes (0.210 g for Model 2.33:1 and 0.286 g for Model 4:1). Notably, in Layer 4 of Model 2.33:1, the CSR increases from approximately 0.30 to 0.35 as the number of cycles increases from 16 to 40, resulting in an average CSR of 0.33 over all 40 cycles.

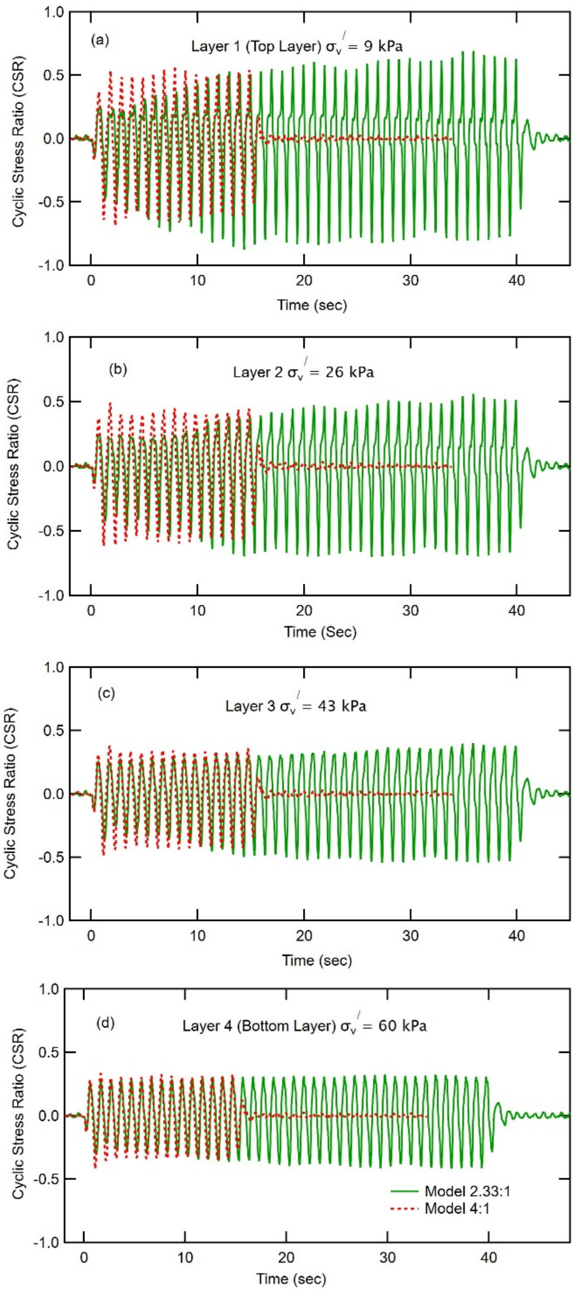

Figure 4. Time Histories of Cyclic Stress Ratio

In the upper half of Model 2.33:1, the CSR time histories exhibit significant variability and are relatively low during the initial cycles. As the number of cycles increases, the CSR values rise substantially. For example, at Layer 2 of Model 2.33:1, the average CSR during the first 15 cycles is 0.41, which is lower than that observed in Model 4:1 at the same depth. However, the average CSR increases to 0.57 between cycles 16 and 40. This trend suggests that the material exhibits dilative behavior, resulting in strength gain with continued cyclic loading. This interpretation is further supported by the evolution of excess pore water pressure discussed in a subsequent section.

For both models, the average CSR decreases with increasing vertical effective stress; in other words, CSR decreases with depth. For the first 15 loading cycles, the average CSR values for Layers 1 through 4 in Model 2.33:1 are 0.54, 0.41, 0.33, and 0.30, respectively, while the corresponding values for Model 4:1 are 0.56, 0.49, 0.38, and 0.32. These results clearly indicate that, for a comparable number of loading cycles, Model 4:1 exhibits higher average CSR values than Model 2.33:1 at all depths.

The influence of vertical effective stress on the average CSR is illustrated in Figure 5. In addition, the effect of the number of loading cycles is evident in the response of Model 2.33:1. As the number of cycles increases from 15 to 40, the CSR increases, with the effect being more pronounced at lower vertical effective stresses (shallower depths). This trend indicates that the material experiences a significant gain in strength at shallow depths as cyclic shaking continues.

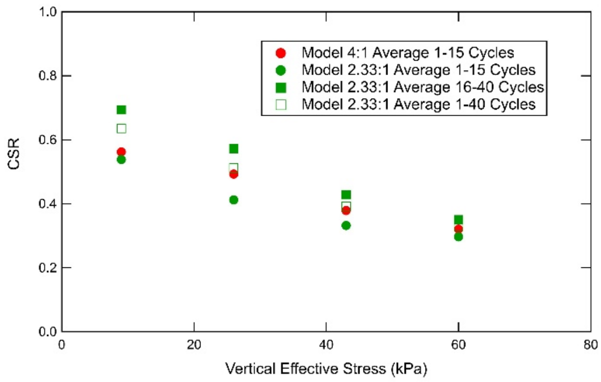

Figure 5. Effects of Vertical Stress on Cyclic Stress Ratio

3.1.2 Cyclic shear strains

The calculated shear strain time histories at each depth for both models are presented in Figure 6. The amplitudes of the cyclic shear strain responses are generally uniform with time. A comparison between the two models shows that the average cyclic shear strain amplitude in Model 2.33:1 is higher than that in Model 4:1, despite the comparable CSR values observed at the bottom layer of both models. This difference can be attributed to several factors. First, Model 2.33:1 likely exhibited lower shear strength and stiffness than Model 4:1 due to its lower gravel content, even though both materials had a similar initial void ratio of approximately 0.70. Second, the generation of excess pore water pressure in Model 2.33:1 was greater than that in Model 4:1, as discussed in detail in the following section. Additionally, Model 4:1 had a slightly higher relative density (Dr ≈ 28.6%) compared to Model 2.33:1 (Dr ≈ 16.3%), suggesting that relative density may have a greater influence on shear strain response than the initial void ratio.

Overall, the average shear strain for Model 4:1 over the first 15 loading cycles is approximately 1.24%. For Model 2.33:1, the average shear strains over the first 15 cycles and over 40 cycles are approximately 1.57% and 1.63%, respectively. For both models, the shear strains in the upper half of the model are slightly lower than those in the lower half.

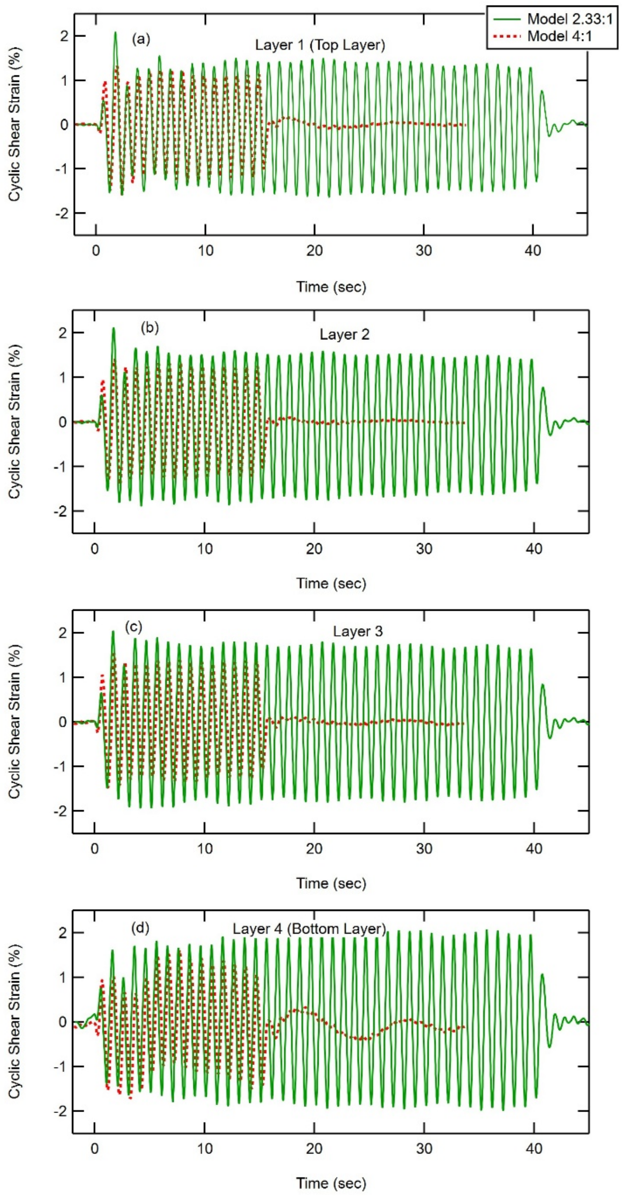

Figure 6. Time Histories of Cyclic Shear Strain

3.1.3 Stress-strain loops

Shear stress-shear strain behaviors are further evaluated in Figure 7. The behavior at the bottom layer show that the soils in both models are relatively close in stiffness, and the stress-strain loops have less distortion compared to other layers. Higher shear strain in the Model 2.33:1 is again clearly observed in the figure while the CSR is close in the bottom layer. The stress-strain loops for both models clearly distort for all other layers, with the greatest distortion observed in the shallower soil layer. This is likely related to the low effective stress for this layer in which the soil is allowed to dilate more easily. As mentioned, the shear strain at the top half of the models is lower than the bottom half of the model, this could possibly relate to the distortion of the stress-strain loops as when the shear stress increases significantly while the shear strain remains nearly same. This behavior implies that the soil gains more stiffness as it exhibits dilative behavior at higher strains and during the shear stress reversal. For all soil layers, the Model 2.33:1 shows higher reduction in stiffness and possible higher damping in comparison with the Model 4:1. Due to higher amount of sand, the average size of soil particles is smaller. Therefore, the sample has higher potential to move or roll over each other under cyclic loading, resulting in higher damping.

3.2 Impact of Number of Cycle on Excess Pore Water Pressure and Volume Change

The development of pore water pressure during shaking for both models is presented in Figure 8. For all soil layers, Model 2.33:1 generated higher excess pore water pressure than Model 4:1. Despite having comparable initial void ratios, the higher excess pore water pressure observed in Model 2.33:1 is likely attributable to its lower permeability resulting from the higher sand content.

In Model 4:1, the pore water pressure response was transient, characterized by oscillations during shaking and no accumulation of excess pore water pressure over successive loading cycles. The maximum positive pore water pressure ratio (Ru), defined as the ratio of excess pore water pressure to the effective vertical stress, was approximately 0.56, observed at Cycle 3 in Layer 2. The Ru amplitudes decreased slightly with increasing number of cycles across all layers, and no residual pore water pressure was observed either between loading cycles or after the shaking ended.

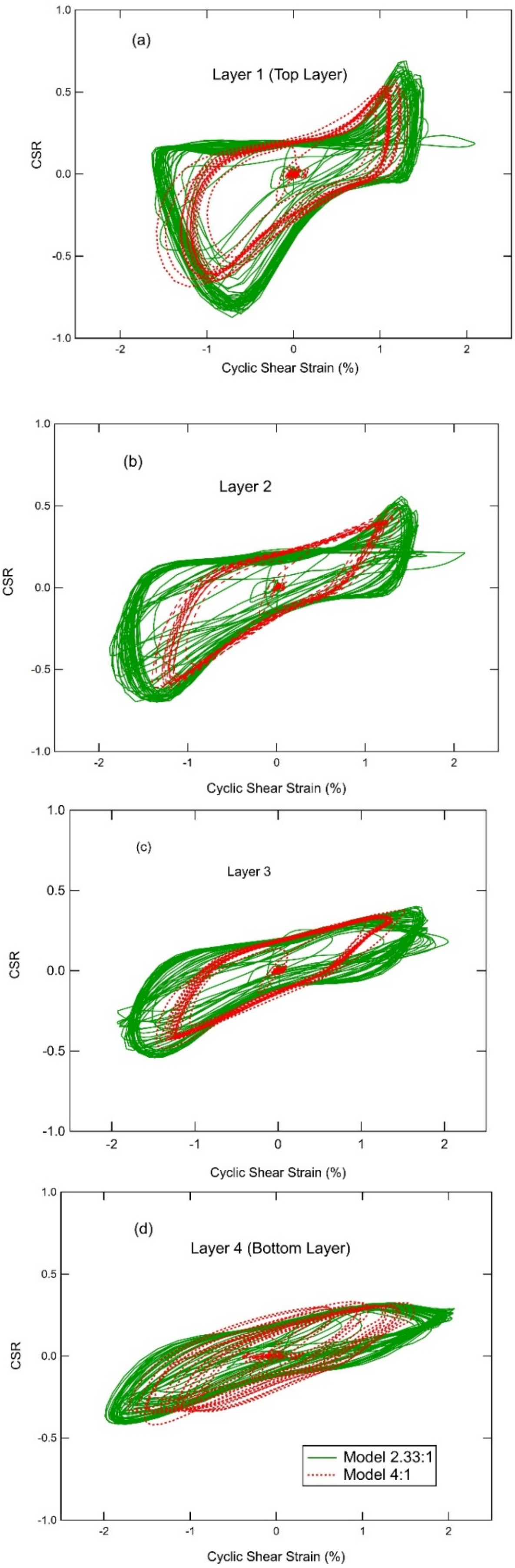

Figure 7. Comparison of Stress-Strain Loops

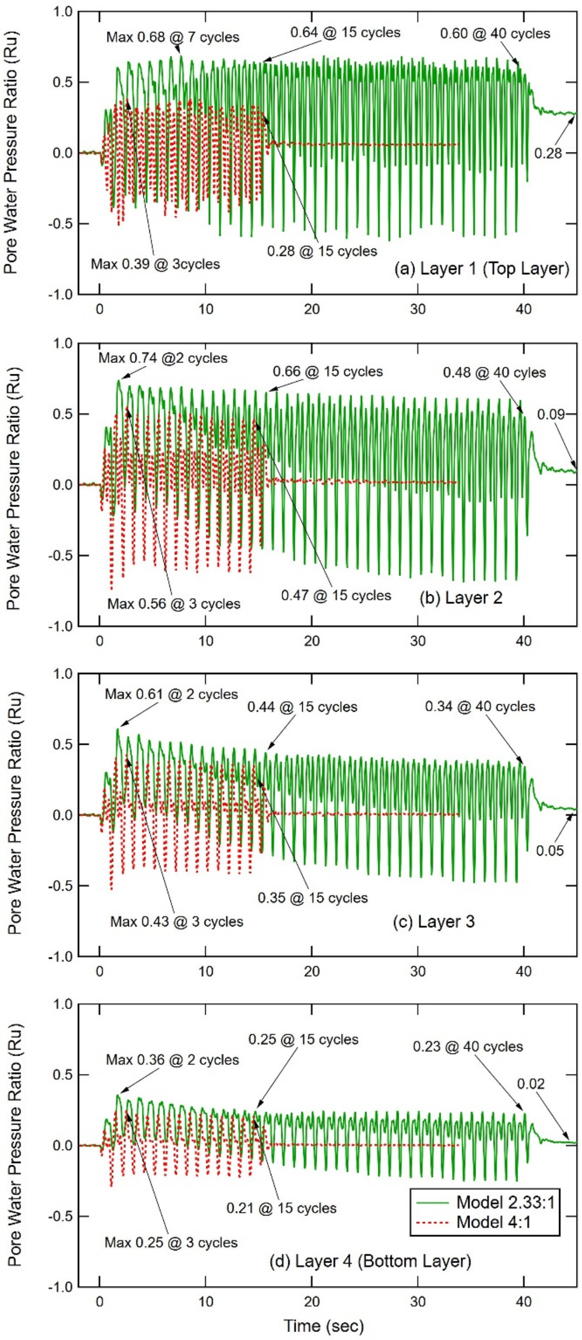

Figure 8. Pore Water Pressure Development

In contrast, some accumulated excess pore water pressure was observed in Model 2.33:1, particularly in the upper half of the model. The maximum Ru occurred at Layer 2. Despite the higher shaking amplitude and greater number of loading cycles applied to this model, Ru reached a peak value of 0.74 at Cycle 2, followed by gradual dissipation as shaking continued. The Ru values decreased to 0.66 and 0.60 at Cycle Numbers 15 and 40, respectively. Based on a liquefaction criterion of Ru > 0.95, liquefaction did not occur in this model. After the shaking ended, pore water pressure dissipated rapidly, with Ru decreasing to approximately 0.09. At the top layer of Model 2.33:1, Ru was slightly lower than that of the underlying layer during shaking and reduced to approximately 0.28 after shaking. In the lower half of Model 2.33:1, excess pore water pressure dissipated more rapidly during shaking, indicating a more stable response at greater depths.

Both centrifuge models allowed drainage at the surface; consequently, settlement occurred during shaking under partially drained conditions. Surface settlement measurements were used to evaluate the average volumetric strain of the entire model. The evolution of volumetric strain with increasing number of loading cycles is presented in Figure 9.

For Model 4:1, although no residual excess pore water pressure accumulated during individual loading cycles, cyclic loading resulted in soil densification, with a total volumetric strain of 1.15% at the end of shaking. The average void ratio decreased from 0.686 to 0.669, while the D_r increased from 28.6% to 35.7%, corresponding to an increase of approximately 7%. As discussed previously, the relatively low Ru values observed in Model 4:1, together with the transient pore water pressure response (i.e., no accumulated excess pore water pressure), indicate that the observed settlement was primarily caused by seismic compression.

In contrast, Model 2.33:1 exhibited a significantly higher rate of volumetric strain accumulation with increasing number of cycles. The accumulated volumetric strain reached 3.1% and 4.67% at Cycle Numbers 15 and 40, respectively. The average void ratio decreased from 0.685 to 0.670 after 15 cycles and further to 0.640 after 40 cycles. Correspondingly, the D_r increased from 16.3% to 32.9% after 15 cycles and to 43.4% after 40 cycles. Although full liquefaction did not occur, the larger volumetric strains observed in Model 2.33:1 are attributed to the higher magnitude and accumulation of excess pore water pressure, which resulted in larger cyclic shear strains, as discussed previously. While the soil did not reach a liquefied state, the magnitude and behavior of excess pore water pressure likely caused partial loss of structure, leading to volume change through a combination of seismic compression and reconsolidation settlement. In addition, as shown in Figure 7, although the stiffness of both models was comparable at the bottom layer, the stiffness of Model 2.33:1 in the upper half of the model was greater than that of Model 4:1 at higher numbers of shaking cycles. This behavior is attributed to the higher relative density achieved in Model 2.33:1 by the end of the 40 loading cycles.

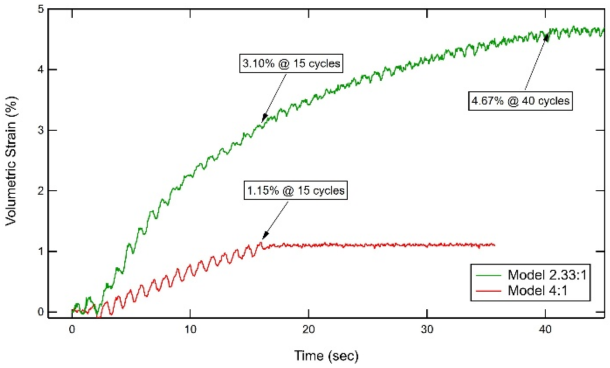

Figure 9. Evolution of Volumetric Strain

Overall, results from both centrifuge tests indicate that even with identical initial void ratios, material composition—specifically the gravel-to-sand ratio—has a significant influence on pore water pressure response, which in turn governs the resulting volumetric strain behavior of saturated mine waste rock. In waste rock with a high gravel-to-sand ratio and higher permeability, volume change is expected to be governed primarily by seismic compression and reconsolidation settlement.

4 CONCLUSIONS

This paper presents the centrifuge model preparation and dynamic testing of two waste rock samples with gravel-to-sand ratios of 2.33:1 and 4:1 by weight. Although different base acceleration amplitudes were applied to each model, the cyclic stress ratio at the base of both models was approximately 0.30. Results from both tests indicate that CSR increases with decreasing effective stress. Compared to Model 4:1, lower CSR values were observed in Model 2.33:1 due to a greater reduction in soil stiffness. Model 2.33:1 also exhibited higher excess pore water pressure generation, leading to larger cyclic shear strains and increased damping. In contrast, although excess pore water pressure developed in Model 4:1, no residual pore pressure accumulated with increasing number of cycles. Dilative behavior at low effective stress was observed in both models. Due to the higher magnitude and accumulation of excess pore water pressure, Model 2.33:1 experienced greater loss of strength and stiffness, resulting in more than twice the volumetric strain observed in Model 4:1. Overall, the results demonstrate that soil composition significantly influences relative density and permeability, which in turn govern the dynamic response of waste rock. A difference of only 10% by weight in gravel and sand content was shown to produce substantial differences in dynamic behavior.

REFERENCES

Antonaki, N., Abdoun, T., and Sasanakul, I. 2017. Consolidation and dynamic response of a layered mine tailings deposit in centrifuge tests. *Geotechnical Testing Journal*, *40*(5).

Antonaki, N., Abdoun, T., and Sasanakul, I. 2018. Centrifuge tests on comixing of mine tailings and waste rock. *Journal of Geotechnical and Geoenvironmental Engineering*, 144(1), 04017099.

Brennan, A. J., Thusyanthan, N. I., and Madabhushi, S. P. 2005. Evaluation of shear modulus and damping in dynamic centrifuge tests. *Journal of Geotechnical and Geoenvironmental Engineering*, 131(12), 1488-1497.

Elgamal, A., Yang, Z., Lai, T., Kutter, B. L., and Wilson, D. W. 2005. Dynamic response of saturated dense sand in laminated centrifuge container. *Journal of Geotechnical and Geoenvironmental Engineering*, 131(5), 598-609.

Rayhani, M. H. T., and El Naggar, M. H. 2008. Dynamic properties of soft clay and loose sand from seismic centrifuge tests. *Geotechnical and Geological Engineering*, 26, 593-602.

Ruttithivaphanich, P., and Sasanakul, I. 2022. Centrifuge modeling studies on effects of composition on liquefaction of mine waste rock. *Soil Dynamics and Earthquake Engineering*, 160, 107378.

Ruttithivaphanich, P., and Sasanakul, I. 2023. Centrifuge Modeling of Fines Content Influence on Liquefaction Behaviors of Loose Gravelly Soils. *Journal of Geotechnical and Geoenvironmental Engineering*, *149*(3), 04023008.

Salam, S. 2020. Cyclic Behavior of Fine Coal Refuse and Seismic Stability of Coal Tailings Dams. Ph.D. Thesis, The Pennsylvania State University.

Sorta, A. R. 2015. Centrifugal Modelling of Oil Sands Tailings Consolidation. Ph.D. Thesis, University of Alberta, Department of Civil and Environmental, Edmonton, AB, Canada.

Zeghal, M., Elgamal, A. W., and Parra, E. 1996. Identification and modeling of earthquake ground response—II. Site liquefaction. *Soil Dynamics and Earthquake Engineering*, 15(8), 523-547.